IL NUOVO CIMENTO **41 C** (2018) 184
DOI 10.1393/ncc/i2018-18184-6

Colloquia: IWM-EC 2018

Isospin transport properties in nuclear matter: Light clusters as isospin tracker

M. Henri, O. Lopez and D. Durand

LPC Caen, Normandie Univ., ENSICAEN, UNICAEN, CNRS/IN2P3 - 14000 Caen, France

received 3 December 2018

Summary. — The study of transport properties is a key point to determine energy dissipation and isospin transport for heavy-ion–induced collisions in the Fermi energy domain. This can be achieved by measuring the nuclear stopping linked to the in-medium mean free path λ^*_{NN} of nucleons in nuclear matter. The quantities are also a good probe to constrain the phenomenological and theoretical models of the nucleon-nucleon interaction in nuclear matter. In this talk, we present new simulations for light $A = 3$ clusters (^{3}H, ^{3}He) compared to experimental data on a large-scale analysis, coming from the INDRA 4π array. By looking at the velocities distributions of the light clusters, we demonstrate that we are able to get consistent information concerning the transport properties of nucleons in nuclear matter.

1. – Introduction

Over the last decades, the equation of state (EoS) of asymmetric nuclear matter has been widely studied in order to bring constraints on theoretical models that aim to describe for example core collapse supernovae or neutron star structure [1]. Heavy-ion collisions (HIC) at intermediate energies are the unique tool that allows to bring the system in conditions near to the ones experienced in astrophysical objects. Thanks to these experimental data, various observables can be used to constrain the existing formulation of the EoS, like isoscaling or imbalance ratio.

In the study presented in this work, we use the light $A = 3$ isobaric clusters to study isospin transport in central HIC. Indeed, the ^{3}H ($\frac{N}{Z} = 2$) and the ^{3}He ($\frac{N}{Z} = 0.5$) present an important $\frac{N}{Z}$ difference and should be sensitive to the isospin content of the nuclei of the entrance channel. Beside the isospin study, we also investigate the clusters production in nuclear matter and the link which exists with the transport properties.

From an experimental point of view, we used for the study, part of the systems available in the INDRA database. Those systems and their relevant information are listed in table I for both cluster production and isospin studies.

TABLE I. – *List of the systems used in the cluster production and in the isospin study. Relevant information as the incident energies of the projectile in the production study or the total system asymmetry for the isospin study are precised.*

Production study		Isospin study	
System	Energies (MeV/A)	System (32 MeV/A)	δ
^{58}Ni + ^{58}Ni	32,52,64,90	^{136}Xe + ^{124}Sn	0.20
^{129}Xe + ^{119}Sn	32,50	^{136}Xe + ^{112}Sn	0.16
^{129}Xe + ^{124}Sn	65,80	^{124}Xe + ^{124}Sn	0.16
^{197}Au + ^{197}Au	40,60,80	^{124}Xe + ^{112}Sn	0.12

In this contribution, we present the results we obtained about the cluster production and the isospin transport studies thanks to a combinatorial coalescence model and the experimental data from INDRA.

2. – Experimental data and model

2˙1. *Central events selection on experimental data.* – The experimental data that have been used for the study presented in this paper were acquired thanks to the INDRA [2] 4π array, in operation at GANIL since 1993. For this work we are only considering central collisions, selected using the method proposed in ref. [3] based on the multiplicity. With this selection we usually keep between 1 and 2% of the detected cross-section.

2˙2. *Combinatorial coalescence model.* – In order to study the production of ^{3}H and ^{3}He $A = 3$ clusters, we developed a combinatorial coalescence model. The model is based on the simulation of the HIC in the center of mass of the reaction, at impact parameter $b = 0$. The nucleons composing the two nuclei of the entrance channel (projectile (Z_P, A_P) and target (Z_T, A_T)) are sampled on a Fermi-Dirac distribution at zero temperature, in the momentum space. The two Fermi spheres are separated in the P-space by their relative momentum.

Three nucleons are then randomly chosen among all the available nucleons, and they are brought in the frame of the cluster $(Z_C, A_C = 3)$ where Z_C and $A_C = 3$ are, respectively, the number of protons and nucleons of the cluster. Once these three nucleons formed a cluster, we compute their mean internal energy $\langle E \rangle$ which reads

$$\langle E \rangle = \frac{\sum_{i=1}^{A_C} E_i}{A_C}, \tag{1}$$

where E_i is the energy of the nucleon i.

The coalescence process is supposed to occur before the deexcitation phase of the collision, it is then necessary to consider the final-state interaction between clusters and the fragments. In this combinatorial coalescence model we choose to simulate the fragments using a uniform charged sphere (Z_S, A_S) where $Z_S = Z_P + Z_T - Z_C$ (respectively, $A_S = A_P + A_T - A_C$) is the number of charge (respectively, nucleons) of the so called "source". This source is in expansion with a velocity v_{exp} in order to simulate the repulsion between all charged fragments. In the position space, the source has a given radius R_S at $t = 0$, computed using the well known relation $R_S(0) = r_0 \times A_S^{1/3}$ with $r_0 = 1.2$ fm.

The formed cluster is then randomly placed in the source at the position $r_C(0)$, and its velocity is computed thanks to the momentum of the nucleons as $v(0) = \sum_{i=1}^{A_C} \frac{p_i}{m}$ with p_i the momentum of the nucleon i and m the nucleon mass.

At each time-step, the electric force between the cluster and the charged sphere is computed by mean of the Gauss theorem: the position, the velocity and the radius of the source are updated. We thus have

$$\left\{ \begin{array}{rcl} \overrightarrow{r_C}\,(t + \mathrm{d}t) & = & \overrightarrow{r_C}\,(t) + \overrightarrow{v_C}\,(t)\,, \\ \overrightarrow{v_C}\,(t + \mathrm{d}t) & = & \overrightarrow{v_C}\,(t) + \dfrac{\overrightarrow{F}\,(r_C) \cdot \mathrm{d}t}{m_C}, \\ \overrightarrow{R_S}\,(t + \mathrm{d}t) & = & \overrightarrow{R_S}\,(t) + v_{exp} \cdot \mathrm{d}t, \end{array} \right. \tag{2}$$

where $\overrightarrow{r_C}$, $\overrightarrow{v_C}$ and m_C are, respectively, the position, the velocity and the mass of the cluster. $\overrightarrow{F}$ is the electric force between the cluster and the source. The propagation is stopped when the electric potential energy is lower than 1 MeV.

2˙3. *Final-distributions construction.* – To constrain the final distribution, and given the fact that $\langle E \rangle$ and v_{exp} are not restricted to a given range of values (the only bound is on the expansion velocity which cannot exceed the projectile velocity: causality) we discretize the $\{\langle E \rangle, v_{exp}\}$ space into slices of 1 MeV and 1 cm/ns. Then, for a given couple $(\langle E \rangle, v_{exp})$ we compare the experimental and simulated (filtered) perpendicular ($v_\perp^{cm}$) and parallel ($v_\parallel^{cm}$) velocities distributions and we get the χ^2 value. The comparison is done only on the forward (positive) part of the distributions, in order to avoid the thresholds issues for the backward (negative) part of the distributions. We are thus able to get the likelihood $\mathcal{L} = \exp\left(-\frac{\chi^2}{2}\right)$ for each couple of values. The following step consists in summing all the distributions of the $\{\langle E \rangle, v_{exp}\}$ space, weighted by the likelihood $\mathcal{L}$ value.

In fig. 1, we present the result of the combinatorial coalescence model on the system ^{129}Xe + ^{119}Sn at 50 MeV/A for ^{3}He. We can see a good agreement between the simulated and the experimental distributions, and this is a good point in favour of this model for the following analysis.

3. – Production of clusters in nuclear matter

We used in this part of the analysis the systems listed in the left part of the table I. For each system we generated 10^6 clusters ^{3}H and ^{3}He, and we got the average internal energy $\langle E \rangle$ by means of the projection of the likelihood map on the $\langle E \rangle$ axis. The results are shown in fig. 2.

First, we do not see a system size dependency of the values that we extract, which is a good thing since the cluster characteristics should not be impacted by the size of the system.

The second observation concerns the trend of the evolution: we can see a clear dependency between the mean internal energy $\langle E \rangle$ and the projectile energy E_P. We can formulate two possible reasons for this increase of the mean internal energy:

i) Effect of the entrance channel: by increasing the projectile energy, the relative momentum between the projectile and the target increases also. So the "distance" in the P-space between all the available nucleons is larger.

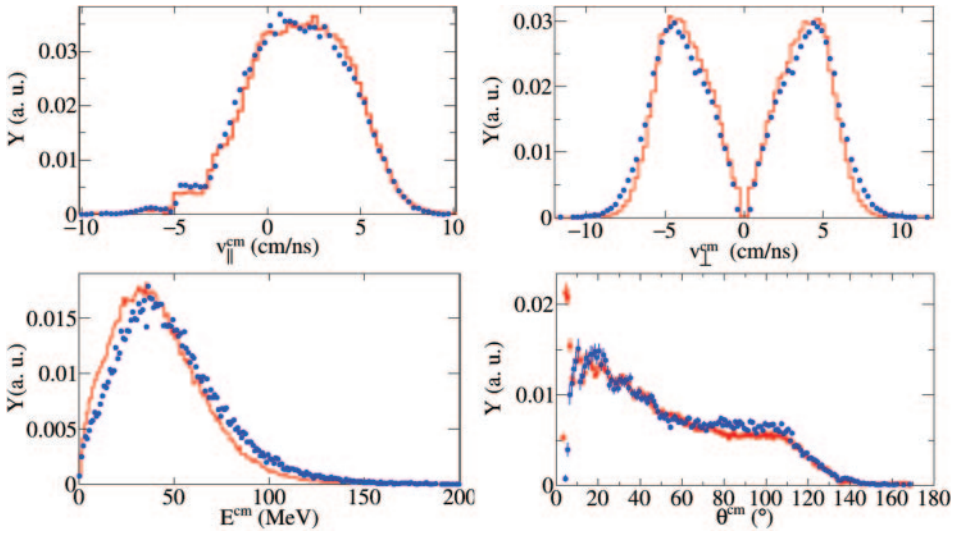

Fig. 1. – (Color online) Results of the combinatorial coalescence model on the system ^{129}Xe + ^{119}Sn at 50 MeV/A for ^{3}He. The blue dots corresponds to the experimental data, while the red histograms corresponds to the simulation. Here the distribution of the parallel (top left) and perpendicular (top right) velocities, the kinetic energy (lower left) and the θ angle (lower right) are presented. All these quantities are in the center-of-mass frame.

ii) In-medium effect: in the entrance channel, the two density distributions of the projectile and the target are fully overlapped (central collisions) which leads to a compression effect. The relative distance between the nucleons in the R-space is smaller, so the relative momentum in P-space increases.

Finally, it would be interesting to compare the values of $\langle E \rangle$ that we obtain in this study to the p_0 momentum of the coalescence approach [4].

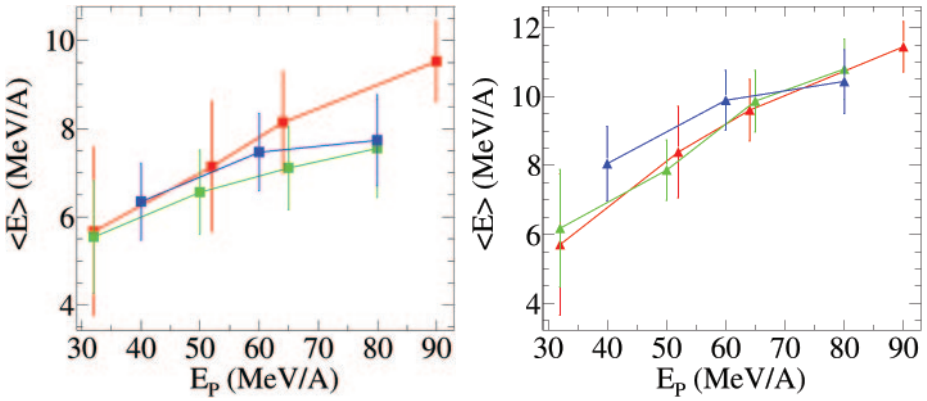

Fig. 2. – (Color online) Evolution of the mean internal energy of the nucleons $\langle E \rangle$ in the cluster as a function of the projectile energy E_P. On the left panel the results concerning ^{3}H, and on the right panel the ones of ^{3}He are shown. The red points corresponds to the ^{58}Ni + ^{58}Ni systems, the green ones to the ^{129}Xe + ^{119,124}Sn systems and the blue ones to ^{197}Au + ^{197}Au.

4. – Isospin transport with $A = 3$ clusters as probes

In this second part of the analysis, we want to address the question of the isospin transport during HIC [5,6]. For that purpose, we used the parallel velocities distributions of ^{3}H and ^{3}He and we introduce the isobaric ratio R_3 which reads

$$R_3 = \frac{\mathbb{V}_{\parallel}\left(^3\mathrm{H}\right)}{\mathbb{V}_{\parallel}\left(^3\mathrm{He}\right)}, \tag{3}$$

where $\mathbb{V}_{\parallel}\left(^3\mathrm{H}\right)$ and $\mathbb{V}_{\parallel}\left(^3\mathrm{He}\right)$ represent the parallel velocities distributions of ^{3}H and ^{3}He in the center-of-mass frame.

From an experimental point of view, the systems that are used for this part of the study are the ones listed in the right part of the table I. For the simulation, we generated 10^6 clusters with the size $A = 3$ without specifying the nature of the wanted cluster. Then, the parallel velocities distributions are constructed and the ratio is computed. The experimental and simulated results are shown in fig. 3.

We see on this figure that the hierarchy and the shapes of the R_3 ratios are the same in the experimental or the simulated data. The more neutron-rich system (blue stars) is above all the other ratios, while the more neutron-poor one (red squares) is below. This indicates us that in the more neutron-rich system, more ^{3}H are produced than in the neutron-poor system, whereas less ^{3}H are produced in the case of the more neutron-poor system.

We focus here on the two other systems, which have the same total number of neutrons and the same total asymmetry (see table I), but where the neutron richness of the projectile and the target is different. We can see in fig. 3 that there is some difference between R_3 ratios in the experimental data when $v_{\parallel}^{cm} > 2\,\mathrm{cm/ns}$, but with this global representation we are not able to see anything on the simulated ratios. We thus introduce

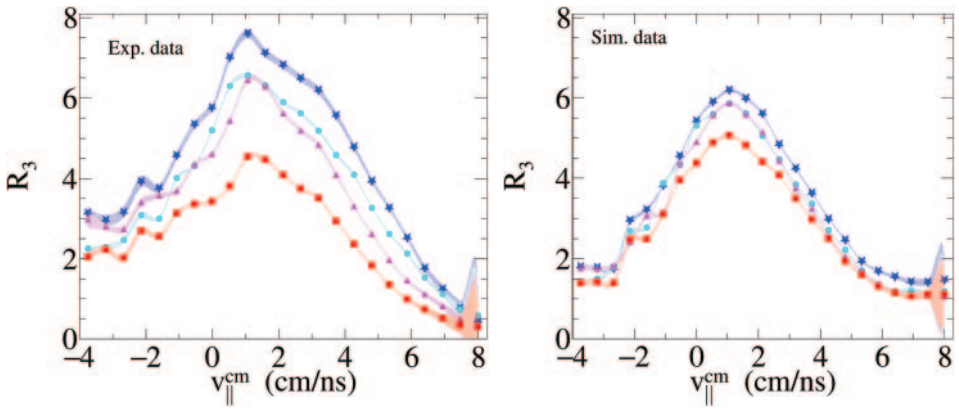

Fig. 3. – (Color online) Distribution of the R_3 isobaric ratios for the four systems used in the isospin transport study. The left panel presents the experimental ratios, while the right one presents the simulated ratios. The blue stars correspond to the more neutron-rich system (^{136}Xe + ^{124}Sn), the red squares to the more neutron-poor one (^{124}Xe + ^{112}Sn). The turquoise dots (^{136}Xe + ^{112}Sn) and the magenta triangles (^{124}Xe + ^{124}Sn) correspond to the systems where the total number of neutrons is the same.

the "normalized" ratios, computed with the following relation:

$$R_3^{norm} = \frac{R_3\,(\mathrm{X})}{R_3\,(^{124}\mathrm{Xe} + {}^{124}\mathrm{Sn})} - 1. \tag{4}$$

If the isospin is fully equilibrated in central collisions, we should see that the R_3^{norm} ratio is the same between the two systems with the same number of neutrons, whatever the richness of the projectile and the target. On the contrary, if the isospin is not fully equilibrated, we should see a deviation between the R_3^{norm} ratios of the two systems.

The results are presented in the fig. 4, where we can see from the experimental side that the isospin seems not to be fully equilibrated in central collisions by using $A = 3$ clusters as probes. Indeed, we can see that the R_3^{norm} ratios of the systems ^{136}Xe + ^{112}Sn (turquoise dots) and ^{124}Xe + ^{124}Sn (magenta triangles) are not superimposed except between 1 and 2 cm/ns. When we look at the simulated data, we observe that the ratios show the same trend when $v_{\parallel}^{cm} > 3$ cm/ns. For lower velocities, we can see that the two ratios are quite the same, this indicating that the simulation seems to equilibrate more largely the isospin compared to what we get from the experimental data.

One important thing to also note is that in figs. 3 and 4 the simulation is able to reproduce the shape and the trend (when $v_{\parallel}^{cm} > 3$ cm/ns) of the ratios R_3 and R_3^{norm} while the experimentally observed amplitude are not reproduced at all. This is for sure related to the numbers of ^{3}H and ^{3}He that are produced by the simulation, and so the production rate of these clusters. We precise here that in the model developed for this work, only the coalescence process has been taken into account. Secondary processes like decay or neutron capture have not been considered, and it may explain the difference observed in the production rate of the clusters. To study this point, we need to use more realistic models, allowing to handle the whole configuration at the same time and not only one cluster per event: it is here necessary to go from an inclusive to an exclusive approach.

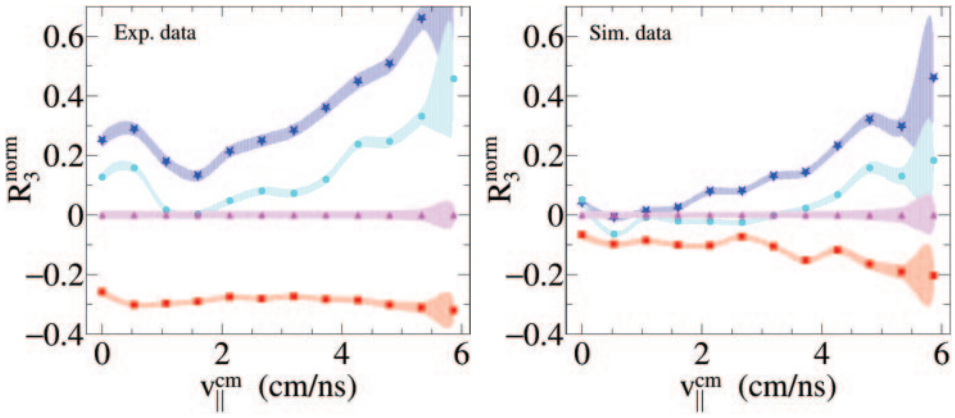

Fig. 4. – (Color online) Distribution of the normalized ratios. Experimental data are presented on the left panel, and simulated ones are presented on the right one. The color code is the same as the one of the fig. 3.

5. – Conclusions and prospects

In this paper, we have presented a new combinatorial coalescence model used to simulate the production of $A = 3$ clusters (^{3}H and ^{3}He) in order to use them as probes for studying the isospin transport properties in the nuclear matter, in central collisions. We saw that our model was able to reproduce the experimental distributions of parallel and perpendicular velocities, but also angular and energy ones.

We first looked at the characteristics of the produced clusters in the nuclear matter, and we showed that the mean internal energy $\langle E \rangle$ increases with the projectile energy.

The second study was devoted to the isospin transport, and we observed that the isospin did not seem completely equilibrated in central collision, when we are using the $A = 3$ clusters as probes. However, we also saw that the effect was very small in the simulated data compared to the experimental ones, and we suppose here that is could be linked with the fact that the simulation is not able to reproduce the production rate of the clusters.

To address this issue, we will continue the study by using use more realistic models which take into account secondary processes like decays or neutron capture. It would also be interesting thanks to the impact parameter available with these models, to observe how our observations evolve by relaxing the centrality condition. Finally, it would be a great advantage in such studies to include heavier fragments in the analysis, and it will be possible soon with the upcoming INDRA-FAZIA coupling at GANIL (Caen) [7-9].

REFERENCES

[1] Margueron J. *et al.*, *Phys. Rev. C*, **97** (2018) 025806.
[2] Pouthas J. *et al.*, *Nucl. Instrum. Methods A*, **357** (1995) 418.
[3] Lehaut G. *et al.*, *Phys. Rev. Let.*, **64** (2010) 232701.
[4] Awes T. C. *et al.*, *Phys. Rev. C*, **24** (1981) 89.
[5] Baran V. *et al.*, *Phys. Rep.*, **410** (2005) 335.
[6] Fable Q., PhD Thesis (2018).
[7] Gulminelli F. *et al.*, Letter of Intent (LOI), SPIRAL2 GANIL (2006).
[8] Valdre S. *et al.*, submitted to *Nucl. Instrum. Methods A*.
[9] Indra-Fazia Collaborations, Proposal for the GANIL PAC (2018).